

Surface properties of ultra-thin tetrahedral amorphous carbon films for magnetic storage technology

C. Casiraghi^{a,*}, A.C. Ferrari^a, R. Ohr^b, D. Chu^c, J. Robertson^a

^aEngineering Department, University of Cambridge, Trumpington Street, Cambridge CB2 1PZ, UK

^bIBM STD Germany, Hechtshsheimerstr. 2, D-55131 Mainz, Germany

^cCambridge Research Laboratory of Epson, Science Park, Cambridge CB4 0FE, UK

Abstract

Diamond-like carbon (DLC) films form a critical protective layer on magnetic hard disks and their reading heads. Film thickness below 2 nm and roughness well below 1 nm are needed for storage density of 200 Gbit/inch². We use atomic force microscopy to study the roughness evolution vs. thickness of highly sp³ hydrogen-free tetrahedral amorphous carbon (ta-C). The roughness of films r generally follows fractal scaling laws, increasing with film thickness h as $r = ah^\beta$, where β is the growth exponent. For a fixed film thickness and scan length l , the roughness varies as l^α , where α is the roughness exponent. We find $\alpha \sim 0.39$ and $\beta \sim 0-0.1$. We performed Monte Carlo simulations, modelling the smoothing effects caused by the thermal spike. The simulation results closely match the experimental findings and define a new growth mechanism for ta-C films. The structural evolution of these ultra-thin films is monitored by Raman spectroscopy. A linear relation between G-peak dispersion and Young's modulus is found. The 2-nm-thick ta-C films are pin-hole free, corrosion resistant, have a Young's Modulus of ~ 100 GPa, sp³ content of $\sim 50\%$ and roughness of ~ 0.12 nm. So, data storage density of 1 Tbit/inch² could be achieved.

© 2003 Elsevier B.V. All rights reserved.

Keywords: Tetrahedral amorphous carbon; Surface characterisation; Coatings; Nucleation

1. Introduction

Hard amorphous carbon films are used in the magnetic storage industry as protective coatings against wear and corrosion. Overcoats currently used are sputtered deposited amorphous carbon films, typically doped with a significant percentage of nitrogen (a-C:N) or hydrogen (a-C:H) and thickness of 3–4 nm [1–5]. The storage density is presently doubling every year. The ultimate barrier to storage density is the super-paramagnetic limit, where the thermal energy is able to overcome the coercive energy of the magnetic bit. For longitudinal recording, this limit is presently approximately 200 Gbit/inch² [1], while vertical recording could allow storage densities up to ~ 1 Tbit/inch² [6]. This requires the read head to approach closer to the magnetic layer and ever-thinner layers of carbon 1–2 nm thick [1,7]. The main role of such ultra-thin films is to provide a

corrosion barrier to the recording medium. They must be atomically smooth, dense, continuous and pin-hole free. However, both magnetron-sputtered a-C:N and a-C:H cease to provide complete protection against corrosion and wear below approximately 2 nm thickness as sputtering is not able to make a continuous film [8]. Highly sp³ hydrogen-free diamond-like carbon (DLC), tetrahedral amorphous carbon (ta-C), are becoming the preferred means of coating read heads [9,10] because of their unique combination of desirable properties, such as high density, atomic smoothness and chemical inertness [11]. Carbon deposited by plasma-enhanced chemical vapour deposition will probably be the industrially preferred method to coat disk.

Ultra-thin ta-C films have been characterised showing how ta-C maintains their desirable properties down to 2 nm thickness [12,13]. However, in order to reach the ultimate storage limits, we must determine the minimum thickness for which ta-C films can be grown continuous and pin-hole free. We therefore need to derive the surface growth mechanism for ta-C films. This is an altogether different problem to the mechanism of sp³

*Corresponding author. Tel.: +44-1223-765242; fax: +44-1223-332662.

E-mail addresses: cc324@eng.cam.ac.uk (C. Casiraghi), jr@eng.cam.ac.uk (J. Robertson).

formation considered in numerous theoretical and experimental studies [14–20]. Indeed, considerable effort has been devoted to the modelling of the formation of DLC and the evolution of the bulk, surface and interface layers on these materials, but not on the issue of the surface formation and the evolution. Only a few groups have studied this problem in various types of carbon films, such as nanostructured carbons [21], some carbon nitrides [22] or hydrogenated amorphous carbons [8]. Some roughness measurements have been reported on thick ta-C films [23,24], showing a correlation between surface roughness and an increase of the film sp² bonding, but they did not analyse the surface evolution.

In this paper we analyse the properties and the kinetic and structural evolution of the ta-C surface. This allows us to quantify the nucleation and the first stages of growth of ta-C films and thereby the ultimate limits of magnetic storage densities.

2. Experimental

Two sets of ta-C films of increasing thickness are investigated:

(1) ta-C films deposited at room temperature in a laboratory scale filtered cathodic vacuum arc (FCVA) with an integrated off-plane double bend (S-bend) [25]. The deposition rate is ~ 0.8 nm/s and the film thickness is between 4 and 70 nm as determined by a combination of deposition rate measurements, ellipsometry and X-ray reflectivity. The deposition chamber was evacuated to 10^{-4} Pa using a turbo molecular pump. No substrate bias was used. The self-bias results in an ion energy of approximately 20–40 eV. ta-C films are deposited on silicon (100) substrates previously cleaned with acetone in an ultrasonic bath. This ensures a substrate roughness of ~ 0.2 nm. Thick samples deposited in these conditions have $\sim 88\%$ sp³, 3.3 g/cm³ density and ~ 750 GPa Young's Modulus [26,27]. Ultra-thin samples deposited in these conditions still exhibit properties of sp³ content $\sim 50\%$, density 2.8 g/cm³ and a Young's Modulus of ~ 100 GPa [12].

(2) ta-C films deposited by a near-production process, filtered high-current pulsed arc (HCA) [28]. The deposition rate is 8–10 nm/s and the film thickness is between 1.6 and 20 nm as determined by X-ray reflectivity and ellipsometry. The base pressure is $\sim 10^{-4}$ Pa. The films were deposited at room temperature on ultra-smooth silicon with roughness of ~ 0.1 nm. Thick samples deposited in these conditions have density ~ 2.9 g/cm³ and Young's Modulus ~ 450 GPa [29]. Ultra-thin samples deposited in these conditions still exhibit ~ 2.6 g/cm³ density and a Young's Modulus of ~ 100 GPa [29].

Note that in magnetic disk coating, the slider magnetic layer is pre-coated with a thin silicon layer to improve

adhesion. Thus, studying the growth on Si substrates can be compared to real industrial process conditions.

The surface morphology evolution was investigated by atomic force microscopy (AFM). We used a Nanoscope III, Digital Instrument AFM in air operating in tapping mode. We used tips made from etched silicon. The resonance frequency and the length of the cantilever are 254–389 kHz and 160 μm , respectively. A surface scan size of $1 \times 1 \mu\text{m}^2$ was used. The root mean square roughness is defined as

$$R = \left[\sum (h_i - h_{\text{ave}})^2 / N \right]^{1/2} \quad (1)$$

where h_i is the film height, h_{ave} is the average of the height values in a given area and N is the number of points. R was calculated on a $0.5 \times 0.5 \mu\text{m}^2$ area in order to avoid any macroparticle [30]. A total of 254 line scans are taken for each image.

Raman measurements were performed with a Renishaw Micro Raman 1000 spectrometer at 633, 514.5 and 244 nm in backscattering geometry. All the UV spectra were corrected by subtracting the system response signal obtained by measuring a background spectrum with an Al mirror and normalising to the atmospheric N₂ vibrations. For samples below 10 nm thickness, UV Raman measurements were performed with long acquisition times (~ 300 s) to allow a good signal to noise ratio and the samples were spun at high speed to avoid any sample damage. The spectra were fitted by using a Lorentzian function for D and T peaks and a Breit-Wigner-Fano (BW F) line shape for the G peak.

3. Experimental results

3.1. Surface analysis

The roughness evolution of a film can generally be described by the fractal scaling laws [31], in which R scales as

$$R \sim l^{\alpha} f(t/l^{\alpha/\beta}) \quad (2)$$

where t is the deposition time with deposition rate assumed constant, l is the length scale, i.e. $l \times l$ is the window size where R is measured, with $l \leq L$ the size of the sample. $f(u)$ is the scaling function of the argument $u = t/l^{\alpha/\beta}$. For small times, i.e. $u \ll 1$, then $R \sim t^{\beta}$ and the heights at different surface sites are independent. As time increases, the heights at different sites become correlated. When the correlations are significant, the roughness saturates at a constant value R_{sat} . α is called the roughness exponent ($0 \leq \alpha \leq 1$). β is called the growth exponent [31]. The exponents α and β uniquely characterise how the surface evolves with the length scale l and the time t . Their values define different

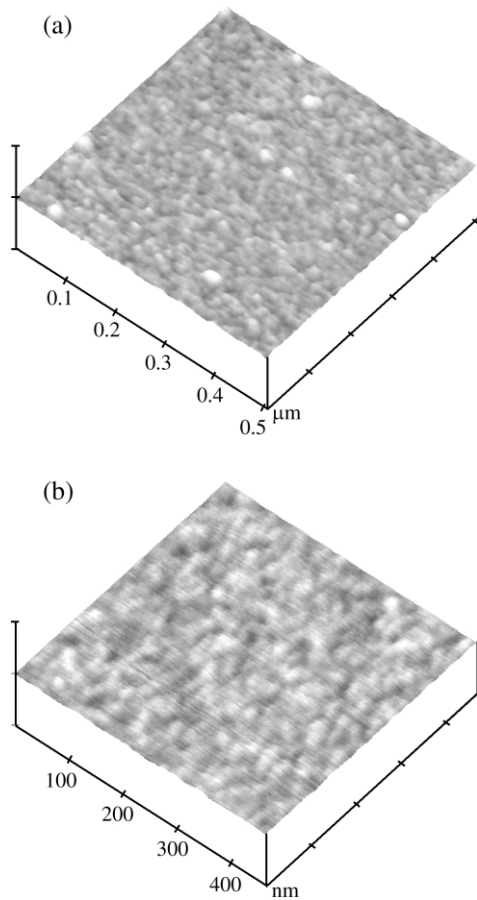


Fig. 1. AFM image of ta-C films with thickness (a) 1 nm deposited by HCA; (b) ~ 70 nm by HCA. The vertical scale is 10 nm.

growth mechanisms universality classes [31,32]. For example, in random deposition the particles stick immediately where they land on a surface and β is 0.5, while α is undefined. In the random deposition with surface diffusion, the particles do not stick irreversibly, but can diffuse to a nearby valley site with lower height. This mechanism gives $\beta = 1/3$ and $\alpha = 1$. For ballistic deposition (with no diffusion), lateral sticking is also allowed, creating overhangs, in contrast to the random deposition model. This gives fractal exponents are $\beta = 0.5$ and $\alpha = 2/3$.

Fig. 1 shows the AFM pictures of 1-nm (HCA) and ~ 70 -nm (FCVA)-thick ta-C films. We note that the surface is continuous and characterised by uniformly distributed features.

Fig. 2 plots the roughness as a function of the thickness. The roughness is almost constant ($R \sim 0.12$ nm) for every sample. The roughness values are in agreement with previous reported data on thicker films [23]. In the case of the FCVA films, the roughness shows an apparent decrease from 0.17 to 0.12 nm when the thickness increases from 4 to 8 nm. This is caused by the initial roughness of the silicon substrate (~ 0.2

nm), which is smoothed exponentially by the covering ultra-smooth ta-C film [33]. The extrinsic origin of this roughness variation for the FCVA films is demonstrated by the roughness trend of the production line HCA samples. No increase is seen, due to the much smoother Si substrate used in this case ($R \sim 0.1$ nm).

The roughness is constant with film thickness in Fig. 2, so the growth exponent β is zero. In addition, the height–height correlation function $H(r,t)$ was determined for different samples against lateral spacing r [34]. The roughness exponent α can be derived from the slope of H against r [31]. We find α between 0.25 and 0.6 (average value is 0.39) [34]. For large r (~ 100 nm), each curve turns into a plateau. The inflection point at which $H(r,t)$ becomes constant with increasing r determines the lateral correlation length ξ [31]. By plotting ξ vs. time, this gives $\beta/\alpha \sim 0.24$ [34]. Using our α value, we find an independent value of β between 0.006 and 0.12. This is in good agreement with β derived directly from thickness scaling in Fig. 2.

Thus, the scaling exponents for ta-C are the growth exponent β between 0 and 0.12 and the roughness exponent $\alpha \sim 0.39$. These exponents do not match any of the existing growth mechanisms, previously described [31], such as the growth continuum equations [35–37].

3.2. Structural and mechanical evolution

The Raman spectra of all carbon systems consist of three features, approximately 1560 cm^{-1} , 1360 cm^{-1} (for visible excitation) and 1060 cm^{-1} (detected only in UV excitation), which are labelled as the G, D and T peaks, respectively [38,39]. The G and D peaks are due to sp^2 sites only. The G peak is due to the bond stretching of all pairs of sp^2 atoms in both rings and chains. The D peak is due to the breathing modes of sp^2 rings. The T peak is due to C–C sp^3 vibrations.

By using different wavelengths and by analysing the

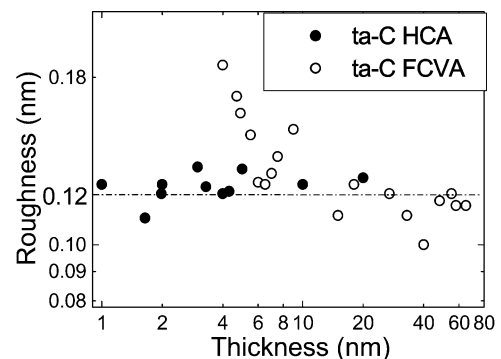


Fig. 2. The Rms surface roughness as a function of the thickness. The roughness is almost constant (~ 0.12 nm). The apparent roughness increase of the thinnest FCVA films is due to the rougher silicon substrate.

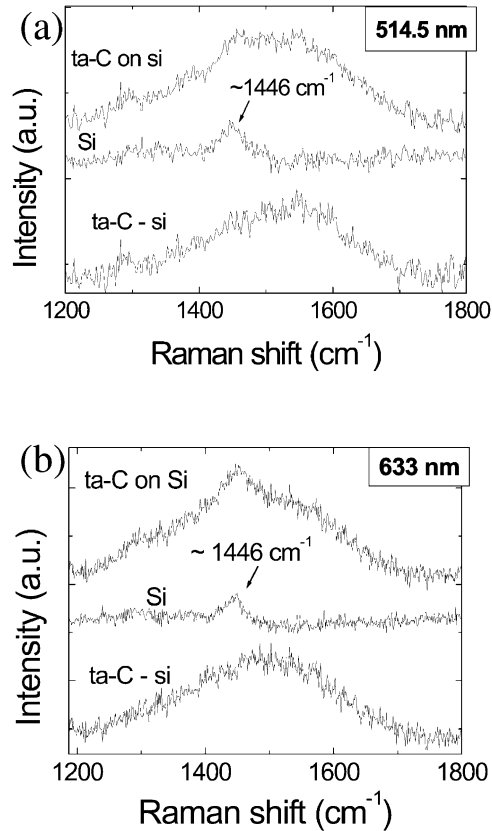


Fig. 3. Effect of the silicon background on the visible Raman spectra of thin ta-C films. The peak at $\sim 1445 \text{ cm}^{-1}$ is the silicon third-order peak as it is detected in the reference silicon spectra [40].

behaviour of the Raman parameters as a function of the excitation wavelength, important additional information is derived on the internal structure of the carbon system [39]. The most useful parameter derived by such an analysis is the dispersion of the G peak. Ref. [39] showed that the G peak positions change in a roughly linear way as a function of the excitation energy. The G peak dispersion was thus defined as the slope of the line connecting the G peak positions measured at different wavelength. The G peak dispersion is a key parameter in order to investigate carbon films since this is proportional to the degree of disorder [39].

To obtain the G peak dispersion we measured our samples at different excitation energies. In order to properly analyse the visible Raman spectra, we must eliminate the contributions of the Si substrate by subtracting the spectrum of the reference un-coated Si. This correction is important since it allows to remove the third-order Si Raman peak at $\sim 1450 \text{ cm}^{-1}$ [40], Fig. 3. For ultra-thin films, this peak is superimposed on the Raman G peak and, unless eliminated, it does not allow a proper fit of the G peak position and, thus, dispersion. Note also that this peak has been previously observed in Raman spectra of thin carbon films, but wrongly

attributed to silicon–carbon vibrations [41]. Indeed, no Si–C vibrations are possible at this frequency [42].

Fig. 4a plots the G dispersion as a function of the film thickness for FCVA and HCA ta-C samples. In both cases, the G dispersion strongly decreases below 10 nm film thickness. The full width half maximum of the G peak decreases from 240 to 170 cm^{-1} at 244 nm excitation and from 360 to 270 cm^{-1} for 633 nm excitation. This implies a decrease of disorder (sp^3 content) and an increase of sp^2 clustering for sub-10 nm films [39]. We thus expect a decrease of the mechanical properties for ultra-thin films as the elastic constants of amorphous carbons scale with the sp^3 fraction and thus with the density [26,27]. Indeed, the Young's Modulus of our films was measured by surface acoustic waves [13,27]. Fig. 4b plots the G peak dispersion as a function of the Young's modulus. A linear relation is found. This demonstrates that the G peak dispersion can assess the mechanical properties of ultra-thin films down to nanometer thickness.

4. Discussion

The AFM measurements have shown that ta-C surfaces are remarkably smooth, and also that the growth exponent β is unusually small ($\beta \sim 0$). To find the origin

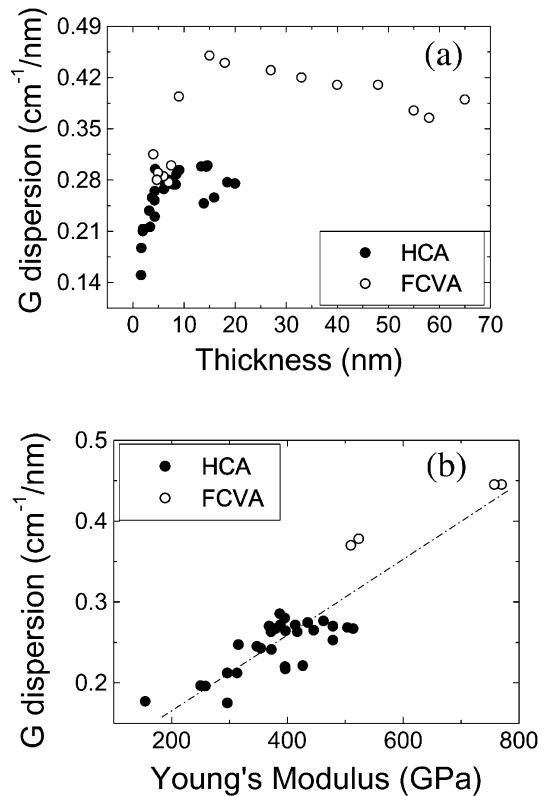


Fig. 4. (a) G peak dispersion as a function of film thickness for FCVA (○) and HCA (●) films. (b) G peak dispersion as a function of Young's modulus. A linear relation is found.

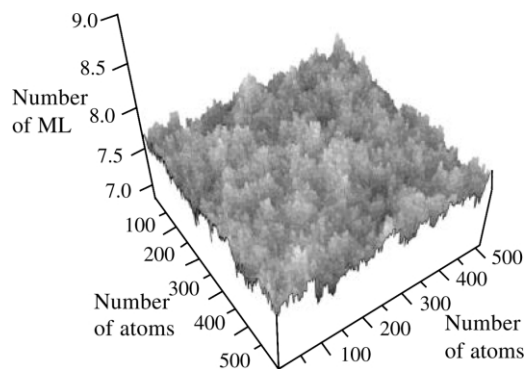


Fig. 5. Simulated surface after thermal spikes cause a flattening to second neighbours of the incident ion. The scaling exponents are $\beta \sim 0.1$ and $\alpha \sim 0.32$.

of this smoothness and investigate the growth mechanism of the ta-C surface, we performed a Monte Carlo simulation. ta-C grows from energetic carbon ions. The generally accepted model for sp^3 formation and ta-C growth is subplantation [11,24]. In this model, two basic processes are assumed to occur: (i) Energetic carbon atoms become incorporated in subsurface positions causing local densification and sp^3 bonding. (ii) A high local temperature associated with the ‘thermal spike’ occurs, due to the excess energy dissipated by the impinging carbon ion.

We consider the thermal spike to be responsible for the surface relaxation during ta-C growth. When the incident ion penetrates the outer atomic layer of the film and goes to the sub-surface layer, its energy is dissipated within a thermal spike volume. This induces the material to locally melt and behave as a liquid. The surface area of the thermal spike becomes locally flat. The only parameter we need to adjust is the number of nearest neighbours affected by the thermal spike. We considered up to three nearest neighbours. We simulated films of increasing thickness (up to 30 monolayers) and with a cell size of 512×512 atoms. We find that β is between 0.08 (first neighbors) and 0.15 (third neighbors). The roughness exponent α slowly increases as the number of nearest neighbours increases. We thus find α is between 0.26 (first neighbours) and 0.36 (third neighbours), in good agreement with experimental data. A simulated surface is shown in Fig. 5.

While the roughness is constant for decreasing thickness, the Raman spectra show that below 10 nm the ta-C structure changes and the mechanical properties become poorer. This can be understood if one considers the cross-sectional structure of ta-C films [19,26]. The film consists of three layers, an outer layer, a middle ‘bulk’ layer and an interfacial layer. The outer surface layer is approximately 0.5 nm thick and is more sp^2 like. Its thickness corresponds to the carbon ion range. There is also an interfacial layer between the C and the

Si substrate, where ion mixing creates C–Si bonding. Since the deposition conditions are constant during film deposition, the thickness of the surface and interface layers is roughly independent of the total film thickness [26]. Thus, for thinner films, the thickness of the middle ‘bulk’ layer decreases, but the nature of the surface layer (and thus the roughness) should not change much with thickness, for a given ion energy. The surface layer is also softer than a layer of similar density in the bulk film. This is also true for the interface layer, as C–Si bonds are softer than C–C bonds. This explains the quick decrease of the mechanical properties once the width of the bulk layer becomes negligible [29].

Fig. 4a also shows that the G peak dispersion goes from 0.45 to $0.2 \text{ cm}^{-1} \text{ nm}$ for S-bend FCVA ta-C films, whilst it moves from 0.28 to $0.1 \text{ cm}^{-1} \text{ nm}$ for HCA ta-C films. This means that the lab scale S-bend FCVA ta-C can reach higher densities, sp^3 content and mechanical properties than the production line HCA ta-C, for each thickness. However, HCA films allow better uniformity over large areas and lower macroparticle density. The higher instantaneous deposition rate of HCA films also increases the temperature of the sp^3 to sp^2 transition with respect to S-bend FCVA films [43]. This is important since the process temperature for hard disk deposition is $\sim 200 \text{ }^\circ\text{C}$.

5. Conclusions

We showed that ultra-thin ta-C films are atomically smooth (roughness $\sim 0.12 \text{ nm}$). The roughness exponent α is ~ 0.39 , while the growth exponent β is between 0 and 0.1. A growth mechanism has been proposed to explain these growth exponents, which differ from what is found in other materials. We assume the thermal spike following the carbon ions subsurface implantation to be the main cause for the surface morphology evolution. Our Monte Carlo simulations reproduce well the experimental exponents. This implies that ultra-thin and ultra smooth ta-C films can be grown down to 1–2 nm thickness. Raman spectra show that, although the roughness is constant for decreasing film thickness, there is a structural modification below 10 nm, related to a change in the film cross-sectional composition. However, a 2-nm ta-C film still possesses a Young’s Modulus of $\sim 100 \text{ GPa}$, sp^3 content of $\sim 50\%$ and a 2.8 g/cm^3 . The smoothness and absence of pin-holes give excellent corrosion resistance down to $\sim 1 \text{ nm}$ thickness [44]. Thus, ta-C satisfies all the requirements [6] needed for the ultimate storage density limit of $\sim 1 \text{ Tbit/inch}^2$.

Acknowledgments

The authors thank D. Batchelder, A. Smith, I.R.R. Mendieta of University of Leeds for UV Raman facilities. CC acknowledges funding from EU project CAR-

DECOM. ACF acknowledges funding from the Royal Society.

References

- [1] P.R. Goglia, J. Berkowitz, J. Hoehn, A. Xidis, L. Stover, *Diamond Relat. Mater.* 10 (2001) 271.
- [2] E.C. Cutiongco, D. Li, Y.W. Chung, C.S. Bathia, *IEEE Trans. Magn.* 33 (1997) 938.
- [3] J. Windeln, C. Bram, H.-L. Eckes, et al., *Appl. Surf. Sci.* 179 (2001) 167.
- [4] J. Robertson, *Tribol. Int.* 36 (2003) 405.
- [5] J. Robertson, *Thin Solid Films* 383 (2000) 81.
- [6] R.J. Wood, *IEEE Trans. Mag.* 38 (2002) 1711.
- [7] D. Li, M.U. Guruz, C.S. Bhatia, Y. Chung, *Appl. Phys. Lett.* 81 (2002) 1113.
- [8] R.J. Waltman, H. Zang, A. Khurshudov, et al., *Tribol. Lett.* 12 (2002) 51.
- [9] H. Han, F. Ryan, M. McClure, *Surf. Coat. Technol.* 120 (1999) 579.
- [10] C.S. Bhatia, S. Anders, I.G. Brown, K. Bobb, R. Hsiao, D.B. Bogy, *J. Tribol.* 120 (1998) 795.
- [11] J. Robertson, *Mater. Sci. Eng. Rep. R* 37 (2002) 129.
- [12] M. Beghi, A.C. Ferrari, K.B.K. Teo, et al., *Appl. Phys. Lett.* 81 (2002) 3804.
- [13] D. Schneider, P. Siemroth, T. Schülke, et al., *Surf. Coat. Technol.* 153 (2002) 252.
- [14] Y. Lifshitz, S.R. Kasi, J.W. Rabalais, *Phys. Rev. Lett.* 62 (1989) 1290.
- [15] D.R. McKenzie, D. Muller, B.A. Pailthorpe, *Phys. Rev. Lett.* 67 (1991) 773.
- [16] J. Robertson, *Diamond Relat. Mater.* 2 (1993) 984.
- [17] D.R. McKenzie, D. Muller, B.A. Pailthorpe, *Diamond Relat. Mater.* 3 (1994) 361.
- [18] H.U. Jager, A.Yu. Belov, *Phys. Rev. B* 68 (2003) 024201.
- [19] C.A. Davis, G.A.J. Amaratunga, K.M. Knowles, *Phys. Rev. Lett.* 80 (1998) 3280.
- [20] M.P. Siegal, D.R. Tallant, P.N. Provencio, D.L. Overmyer, R.L. Simpson, L.J. Martinez-Miranda, *Appl. Phys. Lett.* 76 (2000) 3052.
- [21] R. Buzio, E. Gnecco, C. Boragno, et al., *Surf. Sci.* 444 (2000) L1.
- [22] E. Riedo, J. Chevrier, F. Comin, H. Brune, *Surf. Sci.* 477 (2001) 25.
- [23] X. Shi, L. Cheah, J.R. Shi, S. Zun, B.K. Tay, *J. Phys.: Condens. Matter* 11 (1999) 185.
- [24] Y. Lifshitz, G.D. Lempert, E. Grossman, *Phys. Rev. Lett.* 72 (1994) 2753.
- [25] M.C. Polo, J.L. Andujar, A. Hart, J. Robertson, W.I. Milne, *Diamond Relat. Mater.* 9 (2000) 663.
- [26] A.C. Ferrari, A. Libassi, B.K. Tanner, et al., *Phys. Rev. B* 62 (2000) 11089.
- [27] A.C. Ferrari, J. Robertson, M. Beghi, C.E. Bottani, R. Ferulano, R. Pastorelli, *Appl. Phys. Lett.* 75 (1893) 1999.
- [28] Th. Schulke, A. Andres, P. Siemroth, *IEEE Trans. Plasma Sci.* 25 (1997) 660.
- [29] C. Casiraghi, A.C. Ferrari, R. Ohr, et al., *Diamond Relat. Mater.*, this issue.
- [30] K.B.K. Teo, S.E. Rodil, J.T.H. Tsai, A.C. Ferrari, J. Robertson, W.I. Milne, *J. Appl. Phys.* 89 (2001) 3706.
- [31] A.-L. Barabasi, H.E. Stanley, *Fractal Concepts in Surface Growth*, Cambridge University Press, New York, 1995.
- [32] F. Family, *J. Phys. A* 18 (1985) L75.
- [33] O. Rattunde, M. Moseler, A. Hafele, J. Kraft, D. Rieser, H. Haberland, *J. Appl. Phys.* 90 (2001) 3226.
- [34] C. Casiraghi, A.C. Ferrari, R. Ohr, A.J. Flewitt, D. Chu, J. Robertson, *Phys. Rev. Lett.* 91 (2003) 226104.
- [35] M. Kardar, G. Parisi, Y. Zhang, *Phys. Rev. Lett.* 56 (1986) 889.
- [36] S. Edwards, D. Wilkinson, *Proc. R. Soc. Lond. A* 44 (1966) 1039.
- [37] S. Das Sarma, P. Tamborenea, *Phys. Rev. Lett.* 66 (1991) 325.
- [38] A.C. Ferrari, J. Robertson, *Phys. Rev. B* 61 (2000) 14095.
- [39] A.C. Ferrari, J. Robertson, *Phys. Rev. B* 64 (2001) 075414.
- [40] W.P. Acker, B. Yip, D.H. Leach, R.K. Chang, *J. Appl. Phys.* 64 (1988) 2263.
- [41] M.P. Siegal, D.R. Tallant, L.S. Martinez Miranda, J.C. Barbour, R.L. Simpson, D.L. Overmyer, *Phys. Rev. B* 61 (2000) 10451.
- [42] B. Racine, A.C. Ferrari, N.A. Morrison, I. Hutchings, W.I. Milne, J. Robertson, *J. Appl. Phys.* 90 (2001) 5002.
- [43] J. Koskinen, J.P. Hirvonen, J. Keranen, *J. Appl. Phys.* 84 (1998) 648.
- [44] R. Ohr, B. Jacoby, M.v. Gradowski, C. Schug, H. Hilgers, *Surf. Coat. Technol.*, in press.